OKAYAMA University
Earth Science Reports,
Vol. 12, No. 1, 1-5, (2005)

Tin-bearing chalcopyrite and platinum-bearing bismuthinite in the active Tiger chimney, Yonaguni Knoll IV seafloor hydrothermal system, South Okinawa Trough, Japan

Kaul GENA, Hitoshi CHIBA and Katsuo KASE

Department of Earth Sciences, Faculty of Science, Okayama University, Okayama 700-8530, Japan

The active sulfide chimney ore sampled from the flank of the active Tiger chimney in the Yonaguni Knoll IV hydrothermal system, South Okinawa Trough, consists of anhydrite, pyrite, sphalerite, galena, chalcopyrite and bismuthinite. Electron microprobe analyses indicated that the chalcopyrite and bismuthinite contain up to 2.4 wt. % Sn and 1.7 wt. % Pt, respectively. The high Sn-bearing chalcopyrite and Pt-bearing bismuthinite are the first occurrence of such minerals on the submarine hydrothermal systems so far reported. The results confirm that the Sn enters the chalcopyrite as a solid solution towards stannite by the coupled substitution of $Sn^{4+}Fe^{2+}$ for $Fe^{3+}Fe^{3+}$ while Pt enters the bismuthinite structure as a solid solution during rapid growth. The homogenization temperature of the fluid inclusions in anhydrite (220-310°C) and measured end-member temperature of the vent fluids (325°C) indicate that the minerals are precipitated as metastable phases at temperature around 300°C. The Sn-bearing chalcopyrite and Pt-bearing bismuthinite express the original composition of the minerals deposited from a hydrothermal fluid with temperatures of about 300°C.

Keywords: Sn-bearing chalcopyrite,Pt-bearing bismuthinite, Active sulfide Chimney, Yonaguni Knoll IV, Okinawa Trough, seafloor hydrothermal system.

I. Introduction

Since 1998, a lot of seafloor hydrothermal activities and massive sulfide deposits were discovered in the Okinawa Trough. Among them, hydrothermal activity in the southern most part of the Okinawa trough was first discovered during Yokosuka-Shinkai 6500 cruise YK 00-06 (August 2000) and called Yonaguni Knoll IV hydrothermal system (Hsu et al., 2003). The site was revisited during leg 2 of the Yokosuka - Shinkai 6500 cruise YK04-05 (2004). Preliminary mineralogical study indicated that sulfide chimney ores are polymetallic and consist of sphalerite, pyrite, wurtzite, chalcopyrite, galena, tennantite - tetrahedrite series, bornite, covellite, nukudamite, alabandite, stibnite, barite, anhydrite, calcite and rhodochrosite (Suzuki et al., 2005).

Chalcopyrite with up to 2.4 wt. % Sn and bismuthinite with up to 1.7 wt. % Pt occur in an active sulfide chimney ores from the flank of the Tiger chimney field of the Yonaguni Knoll site. Chalcopyrite with high Sn content and bismuthinite with high Pt content have not been reported previously for the submarine hydrothermal systems. We present here the result of mineralogical studies of this active sulfide chimney ore.

II. Tiger chimney in Yonaguni Knoll IV hydrothermal system.

The Tiger chimney is located at 24°50.87`N and 122°42.02`E and at a depth of 1369 m in the Yonaguni Knoll IV hydrothermal system. The chimney field consists of a broad basal mound of fallen dead chimneys fragments that stand 20 m high above the adjacent valley floors of thick sediments. The active chimneys at the summit of the mound emit clear fluids with end-member temperatures of about 300°C while the black smokers on the flanks emit vent fluids with end-member temperatures of 325°C. Six sulfide chimney ores were collected from the Tiger chimney during the Yokosuka - Shinkai 6500 cruise YK04-05. An active sulfide chimney ore collected from the flank of the Tiger chimney was used in this study (Fig. 1a). During the time of sampling, the vent fluid discharging through the orifice of the chimney has an end-member temperature of about 325°C. Bulk chemical analysis of four fresh volcanic rocks from these areas indicated that the rocks are rhyolite with silica content of 71-73 wt. % and total alkalis of 6.6 to 7.7 wt. %.

III. Sample description and ore mineralogy

From macroscopic observation, the ore shows strong

mineralogical variation from the interior to the exterior of the sulfide chimney ore. The average thickness of the chimney's wall is about 4 cm and consists of three distinct zones (Fig. 1b). Zone A (interior) consists predominantly of chalcopyrite while Zone B and Zone C consist mainly of coarse grained pyrite and anhydrite, respectively. The textural relationships between the three zones suggest an abrupt replacement of zone C by zones B and A due to the change of physical chemical environment on transport across the chimney wall (Fig. 1a & 1b).

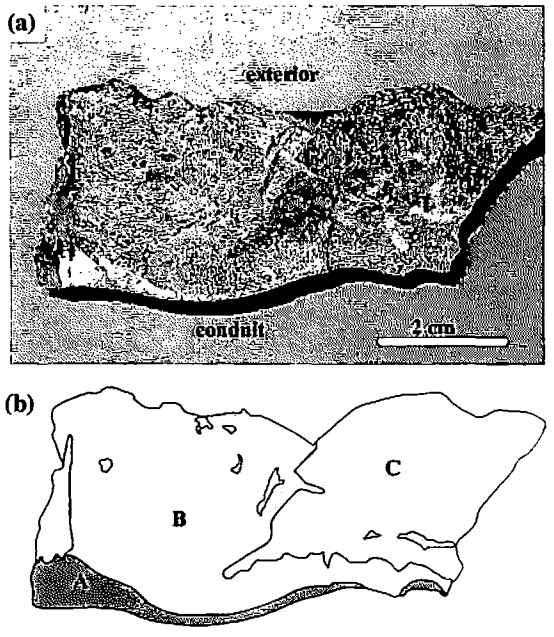

Fig. 1 (a) Photograph of the cross-section of the chimney ore used in this study and (b) Sketch showing the mineralogical zonation seen in the chimney, A: chalcopyrite rich zone, B: pyrite rich zone and C: anhydrite rich zone.

From microscopic observations, the entire chimney ore consists of chalcopyrite, pyrite, sphalerite, galena, bismuthinite and anhydrite. Also, the chimney ore show strong mineralogical zonation from interior to exterior (Fig. 2)

Anhydrite occurs in the exterior of the chimney as coarse grained crystals. It forms radiating sheaves of bladed crystals up to 1mm long and constitutes about 80% of all the minerals in zone C (Fig. 3A). The blackish color of zone C is due to the inclusions of disseminated fine grained sulfide minerals of pyrite, galena and chalcopyrite diseased sphalerite (Fig. 3B). Zone B consists of predominantly coarse grained pyrite (Fig. 3C) with minor amount of bismuthinite with fibrous habit (Fig. 3E). The contact margin between zones A and B is clearly defined by a zigzag (sawtooth) contact morphology (Fig. 3D). Randomly orientated bismuthinite displaying a fibrous habit (Fig. 3E) is interspersed throughout the contact margin of zones A and B (Fig. 3F and Fig. 4)

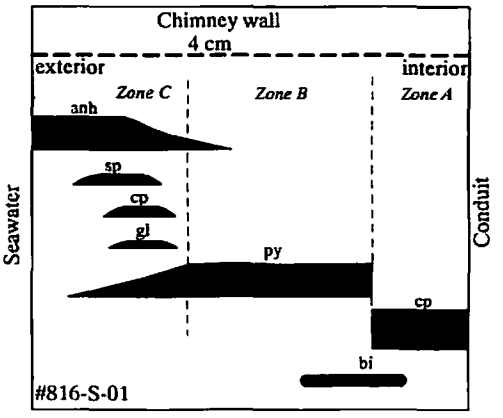

Note: anh = anhydrite, sp = sphalerite, py = pyrite
gl = galena, cp = chalcopyrite, bi = bismuthinite

Fig. 2 Representation of the occurrences of major minerals in the chimney's cross section.

This textural relationship indicates that bismuthinite is deposited later than pyrite and chalcopyrite. The grain sizes of bismuthinite are generally less than 40 μm in diameter and 900 μm in length.

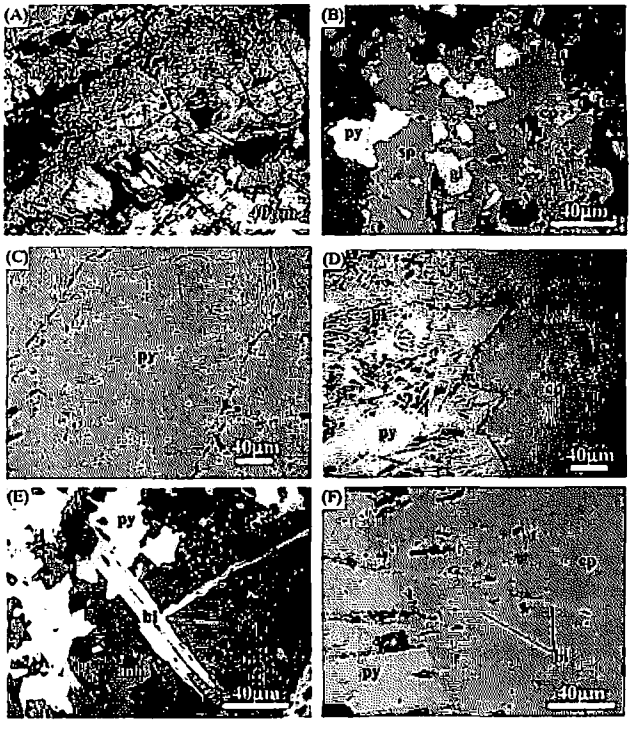

Fig. 3 Photomicrographs illustrating the textures of the minerals in the chimney. (A) Transmitted light photomicrograph of coarse-grained anhydrite in Zone C, (B) Reflected light photomicrograph of fine grained sulfides of pyrite (py), galena (gl), chalcopyrite (cp) and sphalerite (sp) in Zone C, (C) Reflected light microphotograph of coarse grained pyrite in Zone B, (D) Reflected light photomicrograph of zigzag contact margin of Zone A and Zone B, (E) Reflected light photomicrograph of the fibrous bismuthinite (bi) in Zone B, and (F) Reflected light photomicrograph of bismuthinite laths cutting the contact margins of chalcopyrite (Zone A) and pyrite (Zone B).

It was recognized that bismuthinite with fibrous habit is restricted to the contact margins of zones A and B (Fig. 4). Bismuthinite fibers are generally orientated parallel to the growth direction of the chimney walls (Fig. 4).

IV. Result of electron probe microanalyses

The chemical composition of chalcopyrite, pyrite and bismuthinite were obtained by electron probe microanalyser (EPMA), using JEOL-JXA-733 super probe of Okayama University, while the X-ray mapping and back-scattering images of chalcopyrite, pyrite and bismuthinite were obtained by using the automated JEOL-JXA-8600 super probe of Yamagata University. The analytical conditions of EPMA at Okayama University are acceleration voltage of 20kV, a beam current of 20nA and standards of $CuFeS_2$, Bi, Sn and Pt. The analytical results are processed using ZAF correction factor. In addition, the analytical conditions of EPMA at Yamagata University are acceleration voltage of 15 kV, a beam current of 20 nA, ZAF correction factor and standards of ZnS, $CuFeS_2$, Sn, Bi, MnO, Sb_2S_3, Au and Ag. The analytical data of Yamagata University were processed by the on-line computer using sulfide ZAF in the XM-86 PAC program formulated by JEOL.

Fig. 4. Back scattering image of chalcopyrite (cp), pyrite (py) and bismuthinite (bi) along the contact margin of zone A and Zone B. Bismuthinite crystals with fibrous habit are randomly disseminated within the pyrite and chalcopyrite grains.

Electron probe microanalyses indicated that the chalcopyrite, pyrite and bismuthinite contain minor amount of trace elements. The results of chalcopyrite, bismuthinite and pyrite analyzed under these conditions are listed on Tables 1, 2 and 3, respectively.

Fluid inclusion measurement was done for thirty three (33) two phase (liquid + vapor) fluid inclusions hosted by the anhydrite. The homogenization temperatures range from 220° to 310°C, which are slightly lower than the end-member temperature of the vent fluid (325°C). The salinities of the fluid inclusions (2.9 to 4.3 wt. % NaCl equivalent) are consistent with seawater salinity (3.2 wt. % NaCl, Volker et al., 2002). However, some salinities of the fluid inclusion are slightly higher than seawater salinity.

Table 1. Chemical composition of Sn-bearing chalcopyrite

	1	2	3	4	5	6	7	8
Cu	34.61	34.95	35.01	34.42	34.41	34.80	35.13	35.11
Fe	30.26	30.23	29.95	29.24	29.56	29.46	28.12	29.95
Sn	1.20	0.77	0.60	1.94	2.13	1.67	2.40	0.99
Bi	0.19	0.19	0.11	0.04	0.06	0.15	0.00	0.00
S	34.46	34.58	34.49	34.53	34.29	34.71	34.63	34.59
Total	100.72	100.72	100.16	100.18	100.46	100.79	100.28	100.64
Number of atoms per formula unit, based on 8 total atoms.								
Cu	2.01	2.02	2.03	2.01	2.01	2.02	2.05	2.03
Fe	2.00	1.99	1.98	1.94	1.96	1.94	1.87	1.97
Sn	0.04	0.02	0.02	0.06	0.07	0.05	0.07	0.03
Bi	0.00	0.00	0.00	0.00	0.00	0.00	0.00	0.00
S	3.96	3.96	3.97	3.99	3.96	3.99	4.01	3.97
Stannite (wt.%)								
	4.34	2.79	2.17	7.02	7.70	6.04	8.68	3.58

Table 2. Chemical composition of Pt-bearing bismuthinite

	1	2	3	4	5	6
Cu	0.69	0.45	0.80	0.73	0.70	0.76
Fe	0.32	0.45	0.38	0.39	0.28	0.48
Bi	79.19	79.05	79.02	77.62	76.95	77.37
Pt	1.30	1.69	1.54	1.60	1.57	1.66
S	19.17	19.29	18.95	18.91	19.69	19.18
Total	100.67	100.93	100.69	99.25	99.19	99.45
Number of atoms per formula unit, based on 5 total atoms.						
Cu	0.05	0.04	0.06	0.06	0.05	0.06
Fe	0.03	0.04	0.03	0.04	0.02	0.04
Bi	1.89	1.88	1.90	1.88	1.83	1.86
Pt	0.03	0.04	0.04	0.04	0.04	0.04
S	2.99	3.00	2.97	2.98	3.05	3.00

Table 3. Chemical composition of pyrite

	1	2	3	4	5	6
Cu	0.14	0.07	0.00	0.07	0.02	0.08
Fe	47.87	48.05	48.02	47.49	46.63	48.11
Sn	0.00	0.00	0.00	0.00	0.00	0.02
Bi	0.12	0.33	0.50	0.62	1.56	0.00
S	53.27	53.17	53.22	53.46	53.42	52.75
Total	101.40	101.61	101.73	101.64	101.64	100.96
Number of atoms per formula unit, based on 3 total atoms.						
Cu	0.00	0.00	0.00	0.00	0.00	0.00
Fe	1.02	1.02	1.02	1.01	1.00	1.03
Sn	0.00	0.00	0.00	0.00	0.00	0.00
Bi	0.00	0.00	0.00	0.00	0.01	0.00
S	1.98	1.97	1.97	1.98	1.99	1.97

V. Discussion

Sn-bearing chalcopyrite: The chalcopyrite occurs as coarse grained crystal with minor pores and bismuthinite with fibrous habit (Fig. 4). The results of the X-ray

mapping of the chalcopyrite and pyrite along the contact margins of Zone A and B clearly indicate the presence of significant tin in chalcopyrite (Fig. 5A and 5B). Microprobe analysis of chalcopyrite shows a composition of 0.5 to 2.4 % Sn (Table 1). As the tin content increases, the iron content shows a corresponding decrease (Fig. 6). Trace constituent associated with chalcopyrite is bismuth (less than 0.3 wt. %).

The valence state of copper in chalcopyrite and stannite is monovalent (Nakai et al., 1976) while iron in chalcopyrite and tin in stannite are trivalent and tetravalent, respectively (Greenwood and Whifield, 1968). In stannite, iron has to be in a divalent state to maintain a balance of charges while iron is trivalent in chalcopyrite. Mixing of stannite and chalcopyrite would induce coupled substitution of $Sn^{+4}Fe^{+2}$ for $Fe^{+3}Fe^{+3}$. As the Sn content increases in the chalcopyrite of the Tiger chimney ore, there is a corresponding decrease in Fe contents which indicates coupled substitution of $Sn^{4+}Fe^{2+}$ for $Fe^{3+}Fe^{3+}$ in chalcopyrite as a solid solution towards stannite (Fig. 6).

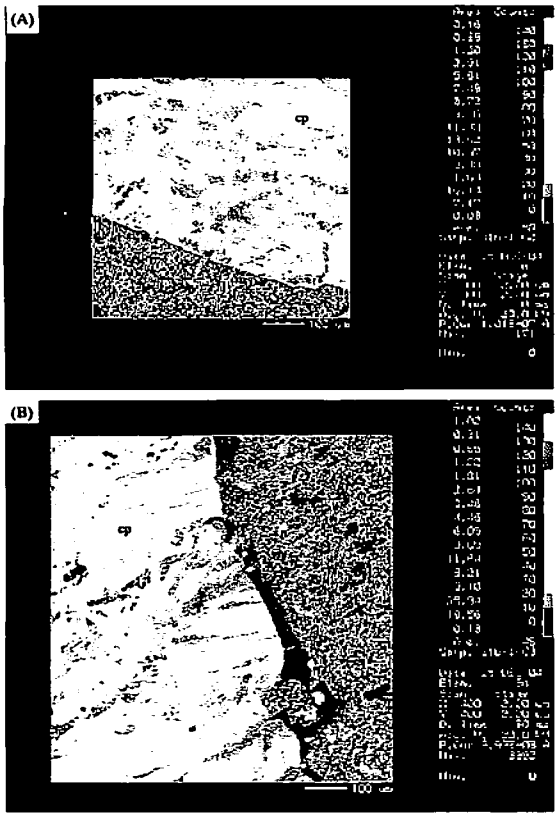

Fig. 5 The X-ray maps showing the distribution of Sn in chalcopyrite and pyrite along the contact margins of zones A and Zone B.

Previous studies (Moh, 1975) showed that only 3 wt. % stannite is soluble in low temperature tetragonal chalcopyrite, which is stable at temperatures below 550°C in the ternary system of Cu-Fe-S (Yund and Kullerd, 1966). However, the solubility of stannite is greater in the high temperature isometric chalcopyrite (>550°C, Moh, 1975). From this study, the maximum Sn content determined by EPMA is about 2.40 wt.% Sn which corresponds to about 8.68 wt. % stannite (Table 1). The end-member temperature of vent fluid (325°C) and fluid inclusion data (220-310°C) indicate that the chalcopyrite with the high Sn content observed in this study precipitated as a metastable phase. The Sn content recognized in this study is exceptionally high. The heterogeneous distribution of Sn in chalcopyrite as observed from the color mapping may indicate the direction of rapid crystal growth (Kase, 1987).

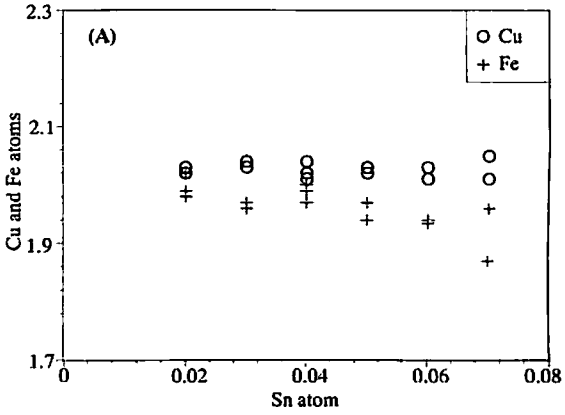

Fig. 6 The number of Cu and of Fe versus the number of Sn in formula unit.

Pt-bearing bismuthinite: The bismuthinite displays a fibrous habit in pyrite and chalcopyrite grains (Fig. 3F and Fig. 4). Microprobe analysis of bismuthinite shows a composition of 1.3 to 1.7 wt. % platinum (Table 2). Trace constituent associated with this mineral is copper (less than 0.9 wt.%) and iron (less than 1.1 wt.%). This is the first reported case of Pt-bearing bismuthinite occurrence on the seafloor hydrothermal systems. The platinum content in the bismuthinite is much higher than the platinum content of hydrothermally precipitated base metal sulfides from the submarine hydrothermal system (< 1wt. %, Hekinian et al., 1980, Koide et al., 1991).

Bismuthian sulfide minerals have never been reported on the seafloor hydrothermal systems apart from minor native bismuth occurrence in sulfide ores from the Escanada Trough, southern Gorda Ridge (Zierenberg et al., 1993). The mode of platinum and copper occurrence in bismuthinite is difficult to deduce from the current data. The presence of both platinum and copper within the bismuthinite may indicate coupled substitution of $Pt^{2+}Cu^{+}$ for Bi^{3+} in the bismuthinite structure. However, there is no positive correlation between Pt^{2+} and Cu^{+} to indicate such substitution. Therefore, the bismuthinite with high Pt content observed in this study probably precipitated as a metastable phase at temperature of 300°C. Chalcopyrite and bismuthinite with such unusual composition have not

been reported in terrestrial deposits. Probably subsequent cooling after deposition and diagenesis may have changed the original composition of the minerals through exsolution.

VI. Conclusion

From this study, the following conclusions can be drawn for minerals in the active sulfide chimney ore from the flank of the Tiger chimney field in the Yonaguni Knoll IV hydrothermal system.

1. Sn-bearing chalcopyrite and Pt- bearing bismuthinite are found in an active sulfide chimney ores from the Yonaguni Knoll IV hydrothermal system. This is the first reported case for the occurrence of such unusual minerals from the submarine hydrothermal systems.
2. Sn content in the chalcopyrite is extremely high (0.51 to 2.4 wt. % Sn). This indicated that the tin enters the chalcopyrite as a solid solution towards stannite by the coupled substitution of $Sn^{4+}Fe^{2+}$ for $Fe^{3+}Fe^{3+}$ in the chalcopyrite structure at temperatures of about 300°C.
3. Pt content in the bismuthinite is also extremely high (1.3 to 1.7 wt. % Pt) compared to those of hydrothermally precipitated base metal sulfides from other submarine hydrothermal systems.
4. The Sn-rich chalcopyrite and Pt-rich bismuthinite are probably precipitated metastably in the Tiger chimney at temperatures around 300°C.

Acknowledgement: We acknowledge financial support from the Japanese Society for the Promotion of Science (JSPS) for the senior author to do his postdoctoral studies at Okayama University. We are grateful for the shipboard scientific party of Yokosuka - Shinkai 6500 cruise YK04-05 (2004) research cruises for their cooperation in sampling. Gratitude is also extended to the operation team of Shinkai 6500 and crew members of RV Yokosuka for their skillful maneuver during sampling. We would like to also acknowledge Professor Kazuo Nakashima of Yamagata University for his assistance with EPMA analysis.

References

Greenwood, N. N. and Whifield, H. J. (1968) Mossbauer effect studies of cubanite ($CuFe_2S_3$) and related iron sulfides. J. Chem. Soc. (A), Inorg. Phys. Theor., 1697-1699.

Hekinian, R., Fevrier, M., Bischoff J. L., Picot P. and Shanks, W. C. (1980) Sulfide deposits from the East Pacific Rise Near 21°N. Science, 207, 1433-1444.

Hsu S-C., Lin F-J., Jeng W-L., Chung Y-C., and Shaw L-M. (2003) Hydrothermal signatures in the southern Okinawa Trough detected by the sequential extraction of settling particles. Marine Chem., 84, 49-66.

Kase K. 1987 Tin-bearing chalcopyrite from the Izumo vein, Toyoha Mine, Hokkaido, Japan. Can. Mineral., 25, 9-13.

Koide, M., Goldberg, E. D., Niemeyer, S., Gerlach, D., Hodge, V., Bertine, K. and Padova, A. (1991) Osmium in marine sediments. Geochim. Cosmochin. Acta, 55, 1641-1648.

Moh, G. H. (1975) Tin containing mineral systems. II Phase relations and mineral assemblages in the Cu-Fe-Sn-S system. Chem. Erde, 34, 1-16.

Nakai, I., Izawa, M., Sugitani, Y., Niwa Y. and Nagashima, K. (1976) X-ray photoelectron spectroscopic study of copper minerals. Mineral. J. (Japan) 8, 135-138.

Suzuki, R., Chiba, H., Ishibashi, J-I. and Gena, K. (2005). Mineralogy and geochemistry of submarine hydrothermal deposits at the Dai-yon Yonaguni Knoll. Society of Resource Geology, 55th Annual Conference, Abstract with Program, P26.

Volker, L., David, A. B. and Peter, H. (2002) Extreme Cr/Br and $\delta^{37}Cl$ isotope fractionation in fluids of modern submarine hydrothermal systems. Mineral. Dep., 37, 765-771.

Yund, R. A. and Kullerd, G. (1966) Thermal stability of assemblages in the Cu-Fe-S system. J. Petrology, 7, 454-488.

Zierenberg, R.A., Koski, R. A., Morton, J. L., Bouse, R. M., and Shanks, W. C. (1993) Genesis of massive sulfide deposits in a sediment–covered spreading center, Escanada trough, southern Gorda Ridge. Econ. Geol., 88, 2069-2098.